



A novel approach for environmentally benign synthesis and solid-state polymerization of fluorinated polyimides in aqueous co-solvent

Sarang Park^{a,b,1}, Yujin So^{a,c,1}, Ki Woong Kim^{a,d}, Jongmin Park^a, Hyun Kim^{a,e},
Lee Kyung Kim^{a,e}, Jinsoo Kim^a, Hee-Tae Jung^c, Dae Woo Kim^{b,*}, Jong Chan Won^{a,e,*}, Yun Ho Kim^{a,e,*}

^a Advanced Functional Polymers Center, Advanced Materials Division, Korea Research Institute of Chemical Technology (KRICT), Daejeon 34114, Republic of Korea

^b Department of Chemical and Biomolecular Engineering, Yonsei University, Seoul 03722, Republic of Korea

^c Department of Chemical and Biomolecular Engineering, Korea Research Institute of Science and Technology (KAIST), Daejeon 34141, Republic of Korea

^d Department of Polymer Engineering, Chungnam National University, Daejeon 34134, Republic of Korea

^e Advanced Materials and Chemical Engineering, KRICT School, Korea National University of Science and Technology (UST), Daejeon 34113, Republic of Korea

ARTICLE INFO

Keywords:

Ecofriendly Process

Fluorinated Polyimide

Aqueous Polymerization

Solid State Polymerization

Transparent Heater

ABSTRACT

This study presents a novel approach that enables an environmentally benign water-based co-solvent synthesis of fluorinated polyimides (FPIs) using conventional fluorine-based monomers such as 4,4'-(hexafluoroisopropylidene)diphthalic anhydride (6FDA) and 2,2'-bis(trifluoromethyl)benzidine (TFMB). The high surface tension inherent in fluorine-based materials, which inhibits water solubility, can be overcome by mixing water with an alcohol-based solvent. The surface tension of the co-solvent decreases proportionally with the alcohol content, facilitating synthesis from fluorine-based monomers that were previously inaccessible in water. Oligomeric fluorinated poly(amic acid) salt (FPAAS) can be rapidly synthesized in aqueous solutions containing alcohol, particularly 1-propanol (PrOH). Subsequent coating and thermal treatment processes allow high molecular weight FPI films to be produced by solid-state polymerization. A comprehensive analysis of the resulting FPI films shows excellent physical properties comparable to conventionally synthesized FPI films. The 6FDA-TFMB-based FPI exhibits remarkable thermal stability up to 570 °C ($T_{d,5\%}$), low yellow index of 1.37, high transparency of 92.9 % and tensile strength of 116.5 MPa. The presented synthetic strategy allows the adoption of monomers with different fluorine-based substituents, thus providing insights for future aqueous synthesis. The thermal, mechanical, and optical qualities of FPIs can be utilized to create optically clear heating devices. The transparent heater, fabricated on the FPI film utilizing a laser patterning technique to create electrodes from silver nanowires, was capable of increasing the temperature up to 100 °C under a 9 V voltage application.

1. Introduction

Polyimide is a highly desirable material due to its exceptional chemical resistance, mechanical properties, and heat resistance. It is widely used in various industries, including automotive, semiconductor, aviation, and marine applications [1,2,3,4,5,6,7]. Fluorinated polyimide (FPI) is a versatile material widely used in various applications, such as displays and transparent films, due to its remarkable physical properties, including high optical transparency, low dielectric constant, and minimal moisture absorption [8,9,10,11,12]. FPI, like other polyimides, is

traditionally synthesized through the formation of poly(amic acid) (PAA), a precursor, in an organic solvent, followed by imidization. The solvents commonly used for this process, such as N-methyl-2-pyrrolidone (NMP), dimethylacetamide (DMAc), and dimethylformamide (DMF), are polar aprotic solvents [13,14,15]. However, these solvents are environmentally hazardous and toxic [16,17,18,19]. Additionally, PAA is susceptible to rapid hydrolysis and exhibits inadequate storage stability [20,21].

To address these limitations, researchers are investigating hydrothermal polymerization as an environmentally friendly method for

* Corresponding authors at: Advanced Functional Polymers Center, Advanced Materials Division, Korea Research Institute of Chemical Technology (KRICT), Daejeon 34114, Republic of Korea.

E-mail addresses: audw1105@yonsei.ac.kr (D. Woo Kim), jcwon@kRICT.re.kr (J. Chan Won), yunho@kRICT.re.kr (Y. Ho Kim).

¹ These authors are equally contributed.

<https://doi.org/10.1016/j.cej.2024.153288>

Received 21 March 2024; Received in revised form 23 May 2024; Accepted 17 June 2024

Available online 18 June 2024

1385-8947/© 2024 The Author(s). Published by Elsevier B.V. This is an open access article under the CC BY-NC-ND license (<http://creativecommons.org/licenses/by-nc-nd/4.0/>).

producing polyimides that does not require organic solvents. This method involves dispersing the main synthetic components, diamine and dianhydride, in water to produce monomer salts, eliminating the need for additional chemicals or catalysts and making it a more eco-friendly option. However, this method presents challenges due to the demanding conditions of high temperature and pressure [22,23,24]. The utilization of water as a solvent for polymerization is a viable alternative to the challenging method mentioned earlier. Aqueous synthesis enables direct production of poly(amic acid) salt (PAAS) precursors that exhibit robust hydrolytic stability compared to PAA. It is worth noting that unlike PAA, which is prone to hydrolysis, PAAS exhibits robust hydrolytic stability. The aqueous polymerization method simplifies the synthesis process for preparing PAAS by enabling one-step synthesis, unlike the traditional two-step organic process of synthesizing PAA and then dissolving it in water. This method also facilitates the production of PAAS with outstanding storage stability, making it an environmentally friendly and efficient technique [25,26,27,28,29]. While it does have an inherent limitation, the benefits of this method make it a highly recommended approach for PAAS synthesis. Aqueous polymerization is limited to monomers with good water solubility, such as 3,3',4,4'-biphenyltetracarboxylic dianhydride (BPDA), p-phenylenediamine (pPDA), and m-tolidine (mTB) [30,31,32,33,34]. Monomers containing fluorine groups or with limited solubility in water are not suitable for aqueous polymerization. Continued research into environmentally friendly synthesis methods for hydrophobic fluorine-based materials in aqueous systems is imperative, as this remains a significant and challenging task.

In this study, we introduce a novel synthesis method for fluorinated polyimides (FPIs) using an aqueous-based co-solvent tailored for typical fluorine-based monomers, such as 4,4'-(hexafluoroisopropylidene)diphthalic anhydride (6FDA) and 2,2'-bis(trifluoromethyl)benzidine (TFMB). Fluorine-based materials inherently possess high surface tension, which hinders their dissolution in water [35]. To overcome this limitation, we developed a co-solvent engineering method by combining water with an alcohol-based solvent, which effectively reduces surface tension. Importantly, the surface tension of the mixed co-solvent decreases proportionally with the alcohol content. This enables the synthesis of fluorine-based monomers that were previously challenging to dissolve in water. Oligomeric FPAAS was successfully synthesized in aqueous solutions containing alcohol, particularly 1-propanol (PrOH). The reaction completed rapidly within one hour. High molecular weight FPI films were achieved through solid-state polymerization by employing a coating process followed by thermal treatment. The thermal, mechanical, and optical properties of the resulting FPI films were analyzed. The physical characteristics were found to be outstanding and comparable to FPI films synthesized using conventional solvents such as NMP. The 6FDA-TFMB-based FPI exhibited remarkable thermal stability with a decomposition temperature of 570 °C ($T_{d,5\%}$), a low yellow index of 1.37, high transparency of 92.9 % at 550 nm, and a tensile strength of 116.5 MPa. By utilizing the outstanding thermal, mechanical, and optical properties of the resulting FPI films, we effectively produce optically transparent and thermally stable interfaces. For example, transparent silver nanowire (AgNW) electrodes can be produced on FPI substrates and then processed with selective laser ablation. The resulting transparent, laser-patterned, selective heating device demonstrates stable heating performance up to 100 °C, indicating potential applications in anti-fogging or defrosting.

Furthermore, we show that the identical mechanism can be utilized for monomers that contain different fluorine-based substituents, such as 2-(trifluoromethyl)-1,4-phenylenediamine (TFMPDA) and 2,2-bis(4-aminophenyl)hexafluoropropane (6FpDA). The combination of an aqueous-based co-solvent with fluorine-based monomers offers new possibilities for eco-friendly FPI synthesis and high-temperature device applications. These findings present a promising solution to address challenges associated with future aqueous synthetic strategies.

2. Experimental section

2.1. Materials

Chemicals were used as purchased, except for 4,4'-(hexafluoroisopropylidene)diphthalic anhydride (6FDA, 99.80 %) which was dried at 190 °C for 10 h in a vacuum after purchase from Changzhou Sunlight Pharmaceutical Co., Ltd. 2,2'-bis(trifluoromethyl)benzidine (TFMB, 99.98 %) and 2-(trifluoromethyl)-1,4-phenylene diamine (TFMPDA, >98.0 %) and 2,2-bis(4-aminophenyl)hexafluoropropane (6FpDA, >98.0 %) purchased from TCI. 4-dimethylaminopyridine (DMAP, 98.0 %) was purchased from Daejung Chemicals and used as received. 1-propanol (PrOH, 99.5+) was purchased from Alfa Aesar. Methyl alcohol (MeOH, 99.5 %), Ethyl alcohol (EtOH, 99.9 %), and 2-propanol (IPA, 99.5 %) were purchased from Samchun Pure Chemical Co., Ltd. N,N-Dimethylacetamide (DMAc, 99.8 %) was purchased from Sigma-Aldrich.

2.2. Synthesis of oligomeric fluorinated PAAS (FPAAS)

A co-solvent was prepared using deionized water and PrOH. The monomers containing fluorine groups were used to synthesize it by varying the mixing ratio of PrOH, which was selected as a cosolvent, and the existing solvent. Co-solvents were created with different water and PrOH ratios, ranging from 10:0 to 0:10. The precursor was then synthesized under a nitrogen atmosphere. DMAP (16.7984 g, 0.1375 mol) was dissolved in a co-solvent in a 250 ml round bottom flask, mixed with TFMB (17.6132 g, 0.055 mol), and stirred at room temperature for 40 min. Subsequently, 6FDA (24.4332 g, 0.055 mol) was added and stirred at 70 °C for 1 h to obtain a 20 wt% oligomeric FPAAS solution. The same procedure was applied to synthesize oligomeric FPAAS using TFMPDA and 6FpDA. The synthesis was performed by adding TFMPDA (5.2842 g, 0.03 mol) and 6FpDA (10.0281 g, 0.03 mol), respectively. At this time, DMAP (9.1628 g, 0.075 mol) and 6FDA (13.3272 g, 0.03 mol) were used together.

2.3. Synthesis of organic-based fluorinated PAA (O-FPAA)

A precursor was synthesized using DMAc as a solvent in a nitrogen atmosphere, similar to oligomeric FPAAS synthesis. TFMB (16.0120 g, 0.05 mol) and DMAc were mixed in a 250 ml round bottom flask and stirred at room temperature for 40 min. Next, 6FDA (22.2120 g, 0.05 mol) was slowly added over a period of 10 min while in an ice bath. The solution was then stirred for 18 h to produce a 20 wt% FPAA solution.

2.4. Preparation of fluorinated polyimide (FPI) film via solid-state polymerization and thermal imidization

The oligomeric FPAAS solution was uniformly coated onto a glass plate to create the FPI film. The solid-state polymerization and thermal imidization process were conducted in a vacuum oven following a temperature and time sequence: 40 °C for 3 h, 80 °C for 1 h, 100 °C for 30 min, 150 °C for 40 min, 200 °C for 40 min, 250 °C for 40 min, and finally 300 °C for 1 h. The heating rate was kept at 1 °C min⁻¹ when rising from room temperature to 40 °C and from 40 °C to 80 °C. Subsequently, the rate was increased to 5 °C min⁻¹ for the subsequent stages. In order to achieve a uniform and excellent FPI film, it is of paramount importance to control the rate of temperature increase during the heat treatment process. The relatively low boiling points of PrOH and water, which are used as solvents, result in the generation of a considerable number of bubbles in the film when the temperature is rapidly increased from a low temperature. Therefore, in the low-temperature heat treatment step, it is important that the solvent is removed slowly at 1 °C min⁻¹.

2.5. Characterization of oligomeric FPAAS and FPI

^1H Nuclear Magnetic Resonance (^1H NMR) spectroscopy was carried out at a concentration of 10 mg ml^{-1} using dimethylsulfoxide- d_6 (DMSO- d_6) and deuterium oxide (D_2O) as solvents on a Bruker advance 500 MHz spectrometer. Fourier Transform Infrared (FT-IR) spectra were collected in the $650\text{--}4,000\text{ cm}^{-1}$ range using a Bruker Alpha-P spectrophotometer in ATR mode. Gel Permeation Chromatography (GPC) was carried out using Shodex columns at $50\text{ }^\circ\text{C}$ with a flow rate of 0.8 ml min^{-1} . Matrix-Assisted Laser Desorption/Ionization Time-of-Flight Mass Spectrometry (MALDI-TOF-MS) analyses were conducted using a Bruker Autoflex Speed TOF/TOF in positive reflector mode. Trans-2-[3-(4-*tert*-butylphenyl)-2-methyl-2-propenylidene]malononitrile (DCTB) was employed as the matrix, and acetone was used as the solvent.

The properties of the prepared FPI film were assessed using the following techniques. Thermogravimetric analysis (TGA) was conducted within a temperature range of room temperature (RT) to $800\text{ }^\circ\text{C}$ at a heating rate of $10\text{ }^\circ\text{C min}^{-1}$ under a nitrogen atmosphere using a Discovery TGA 5500 instrument from TA Instruments. Dynamic mechanical analysis (DMA) was conducted at a rate of $10\text{ }^\circ\text{C min}^{-1}$ within the $\text{RT--}400\text{ }^\circ\text{C}$ temperature range using TA Instruments DMA Q800 equipment. The measurement was conducted at a frequency of 5 Hz and a strain of 0.5% . Universal testing machine (UTM) measurements were performed on tensile specimens prepared in a standard ASTM D882 using Instron's INSTRON 5567 equipment. Each tensile specimen was subjected to a load of 10 kgf at a crosshead speed of 10 mm min^{-1} , and at least five values per specimen were averaged. Grazing Incidence Wide Angle X-ray Scattering (GIWAXS) experiments were performed at the 9A beam-line at the Pohang Accelerator Research Center. The measurements utilized a Mar CCD detector and an X-ray source of 11.08 keV , with the angle of incidence set between $0.10\text{--}0.15^\circ$. Yellow index was measured using a spectrophotometer in $L^*a^*b^*$ color mode according to ASTM E313:96 / KS A 0061:2015 and analyzed using CM-3700d (d/8). Transmittance and haze were measured using haze-grad plus following ASTM D1003 guidelines.

2.6. Fabrication of transparent AgNW electrodes on FPI substrate

The AgNW electrodes were formed on the FPI substrates using a vacuum filtration transfer process [36]. A vacuum pump (MZ 2C NT, VacuuBrand) was connected to a vacuum filter holder (47 mm , LukeGL). Membrane filters composed of nylon filter ($0.2\text{ }\mu\text{m}$, Whatman) and polytetrafluoroethylene (PTFE) filter ($0.2\text{ }\mu\text{m}$, Sterlitech) were placed on top of the holder, then a glass funnel (300 ml LukeGL) was covered. Subsequently, a prepared AgNW solution with a desired density (Flex-iowire2020, SG FLEXIO), which dispersed in ethanol, was poured through the filter. Once the filtration was completed, the AgNWs on the filter can be transferred to a prepared CPI substrate by pressing for 1 min . Laser ablation AgNWs on FPI films was performed using an infrared (IR) pulse laser (M1, Mr Carve) with a wavelength of 1024 nm . The laser scanning path was controlled by laser marker (BslAppSimple, Mr Carve). The laser scanning speed and output power were fixed at 400 mm s^{-1} and 1 W , respectively, with a pulse speed of 30 kHz .

2.7. Characterization of FPI/AgNW heaters

Optical transparency of FPI/AgNW heating devices was measured using a ultraviolet (UV)-vis spectrophotometer (LAMDA 365, PerkinElmer). Surface resistivity of the heating devices was measured using a multimeter (FLUKE-289, FLUKE) and liquid metal (eutectic Gallium-Indium, EGaIn) contacts. For characterizing electrothermal heating properties, copper tapes and wires were attached to ends of the samples such that electrical contact was made to both sides of the film, and a DC power supply (TDP-303B, TOYOTECH) was used for electrical input. Then, IR thermal images were taken an IR camera (E54, FLIR).

3. Results and discussion

We synthesized an oligomeric FPAAS according to the procedure shown in Fig. 1a. A monomer containing a fluorine-based substituent was used to prepare oligomeric FPAAS. 6FDA was fixed with dianhydride and diamines such as TFMB, TFMPDA and 6FpDA were used. Water was selected as the solvent to use an environmentally friendly synthesis method, and a mixture of alcohol solvents was used to increase the solubility of the fluorine-based monomer. DMAP, used as an organic base, helps the dianhydride to dissolve in water by forming a quaternary ammonium carboxylate instead of being converted to carboxylic acid. The synthesized oligomeric FPAAS precursor has a very low molecular weight of $1,000\text{--}2,000\text{ g mol}^{-1}$, which is generally significantly different from the molecular weight of the precursor (PAAS) synthesized by aqueous polymerization [37].

The oligomeric FPAAS is subjected to a thermal imidization process. After the solvent evaporates, an imide structure is formed, and molecular weight amplification occurs through solid-state polymerization, as depicted in Fig. 1b. This can be verified by conducting molecular weight and various structural analyses at different temperatures. The conversion mechanism of oligomeric FPAAS to FPI is similar to the PI conversion mechanism of poly(amic ester) (PAE), a precursor that contains ester groups. The carbonyl carbon of oligomeric FPAAS is attacked by amines. Subsequently, the PrOH that was bonded to the ester is separated, forming an amide group, and imidization ensues. In this process, oligomeric FPAAS acts similarly to PAE, and mechanism analysis was conducted based on the literature [38]. As the temperature increases, a series of reactions occurs rapidly, leading to the formation of high molecular weight polyimide. The solvent evaporates slowly until it reaches its boiling point of $100\text{ }^\circ\text{C}$. After the solvent has completely evaporated, oligomeric FPAAS is converted to FPI through solid-state polymerization, resulting in an increase in molecular weight starting at $150\text{ }^\circ\text{C}$. The experimental section contains a detailed description of the synthesis conditions and thermal imidization process of oligomeric FPAAS salts.

In the early stages of FPI production, we optimized the co-solvent using 4,4'-(hexafluoroisopropylidene)diphthalic anhydride (6FDA) and 2,2'-bis(trifluoromethyl)benzidine (TFMB) as monomers, both of which are widely known monomers with common fluorine-based substituents. The selection of an appropriate co-solvent was crucial and required specific criteria. To enable polymerization in aqueous systems, it was imperative to increase the water solubility of hydrophobic fluorine-based materials. Our approach was guided by the well-established mechanism of interfacial polymerization of PAAS in the presence of organic bases, particularly DMAP [39]. The reaction mechanism is influenced by the solubility and dispersibility of dianhydrides in aqueous media. To facilitate the process, we added a low-surface-tension solvent or surfactants, as outlined in reference. Therefore, we chose to use a water-alcohol co-solvent with low surface tension to improve monomer solubility and accelerate the polymerization process [40].

We experimentally validated this approach using various environmentally friendly basic alcohol-based solvents. From the literature, we observed the surface tension of four mixed solvents of water and alcohol: methanol (MeOH), ethanol (EtOH), 2-propanol (IPA), and 1-propanol (PrOH) [41]. The results indicate a significant reduction in surface tension with the combination of water and alcohol. IPA and PrOH exhibited the most substantial decrease, as shown in Fig. 2a. Both fluorinated monomers dissolved successfully at a polymerization temperature of $70\text{ }^\circ\text{C}$ within 24 h , as depicted in Fig. S1a. The use of alcohol as a co-solvent improved the solubility of the fluorinated monomers, demonstrating the potential for co-solvent-assisted synthesis. The decrease in surface tension was crucial in improving solubility and promoting interactions between reactants, which accelerated the polymerization process.

Various alcohol solvents were used to successfully synthesize oligomeric fluorinated FPAAS for 6FDA-TFMB@DMAP. A homogeneous and colorless precursor solution was achieved through a 1:1 mixture of

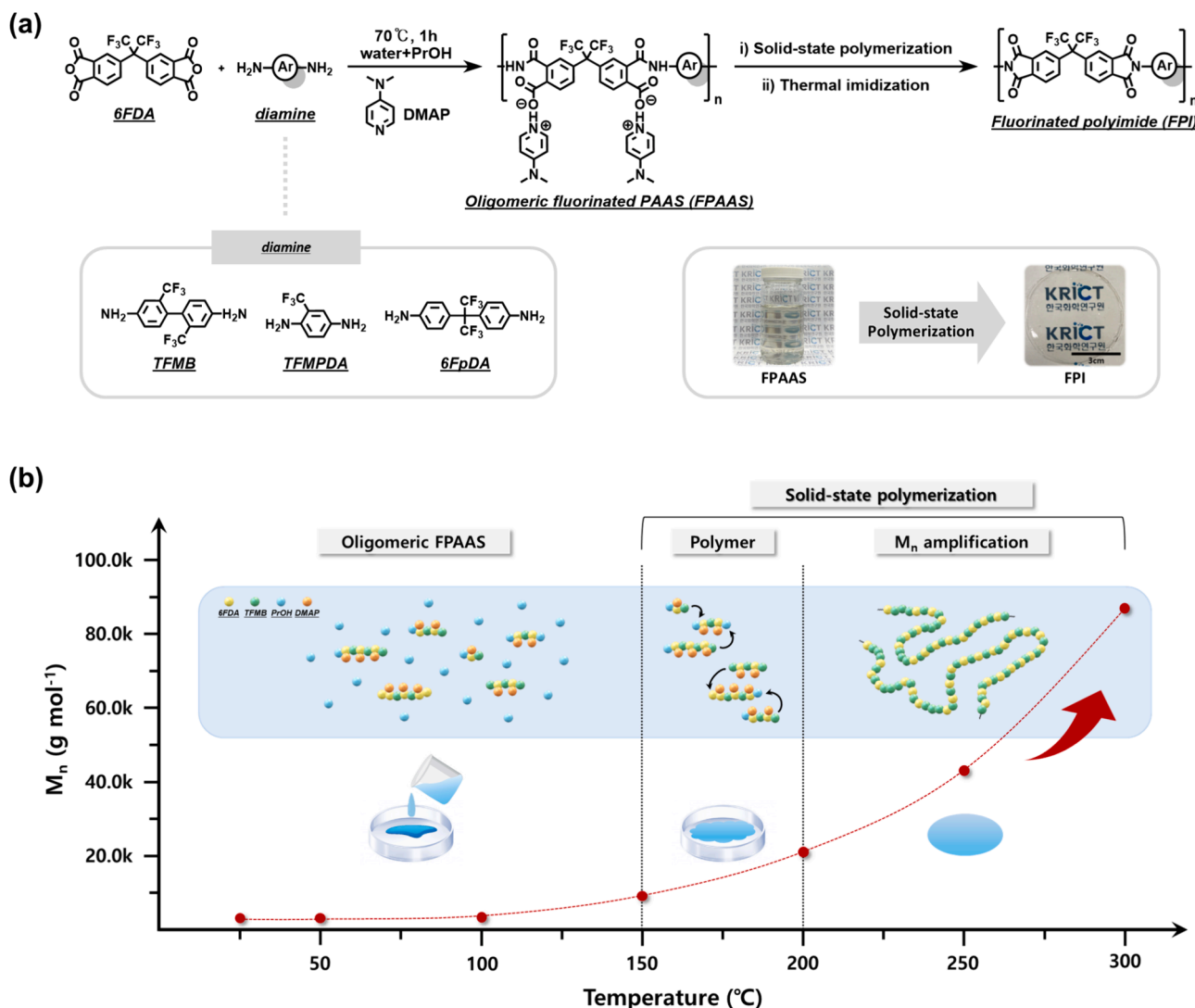


Fig. 1. Schematic representation of the eco-friendly synthetic reaction pathway using a water-alcohol co-solvent. (a) Synthetic scheme illustrating the synthesis of 6FDA-based FPIs with three different fluorine-based diamines: TFMB, TFMPDA, and 6FpDA. (b) Diagram depicting the solid-state polymerization process, transforming oligomeric FPAAS into high molecular weight FPI during thermal treatment.

alcohol and water (Fig. S1b). Structural analysis of the synthesized precursor via ¹H NMR confirmed peak shifts, indicating reactions with the employed monomers (Fig. S1c). The use of the organic base DMAP, with a suitable pK_a value, significantly facilitated the reaction under these conditions, ensuring effective solubility and interactions. The next step in the production of FPI involves the thermal imidization of the precursor. Therefore, it was crucial to select a co-solvent with a boiling point close to that of water. Supplementary Table S1 shows that 1-propanol (PrOH), which has a boiling point of 97 °C, closely matches the boiling point of water at 100 °C. Experiments with four different alcohols as solvents confirmed the impact of boiling point differences on film integrity. The results revealed that film formation becomes increasingly challenging as the boiling point deviates from that of water. In addition, slight differences in the final imide structures were observed, with residual peaks indicating unreacted by-products for EtOH and MeOH compared to PrOH and IPA (Fig. S1d).

Based on these considerations, it was concluded that a mixture of water, PrOH, and IPA in a 1:1 ratio, with a surface tension of approximately 25 mN m⁻¹, would be more efficient for the co-solvent-assisted reaction. In particular, PrOH was identified as the optimal solvent due to its desirable surface tension characteristics and boiling point, consistently yielding uniform films. FPAAS precursors were then

synthesized using a co-solvent composed of PrOH and water. Different ratios of water and PrOH were investigated, as shown in Fig. S2. A colorless and transparent FPAAS solution formed when the PrOH content reached 40 %, but phase separation occurred over time. To ensure consistent production of a homogeneous FPAAS solution, the PrOH content needed to exceed 50 wt%. Therefore, all subsequent experiments used a co-solvent with a 5:5 ratio of water and PrOH, containing the lowest PrOH proportion for consistency. In the event that the PrOH is absent or insufficient, as evidenced by the synthesis result image, the synthesis and FPI production are unfeasible. These observations indicate that PrOH serves as a very important factor in this study.

The oligomeric FPAAS was synthesized using a co-solvent consisting of a 5:5 ratio of water and PrOH. The ¹H NMR analysis of the FPAAS revealed peaks at 4.1 ppm, 1.6 ppm, and 0.9 ppm in Fig. 2b, indicating binding of PrOH to the end of 6FDA within the oligomeric structure. The addition of PrOH also increased the solubility of previously insoluble TFMB, indicating progress in the reaction. Fig. S3 provides additional information on the impact of PrOH on monomers, verifying the successful synthesis of fluorine-based monomers that were previously difficult to synthesize in water. The molecular weight of the oligomeric FPAAS was measured using gel permeation chromatography (GPC) and remained stable at approximately 1200 g mol⁻¹ after 1 h of synthesis.

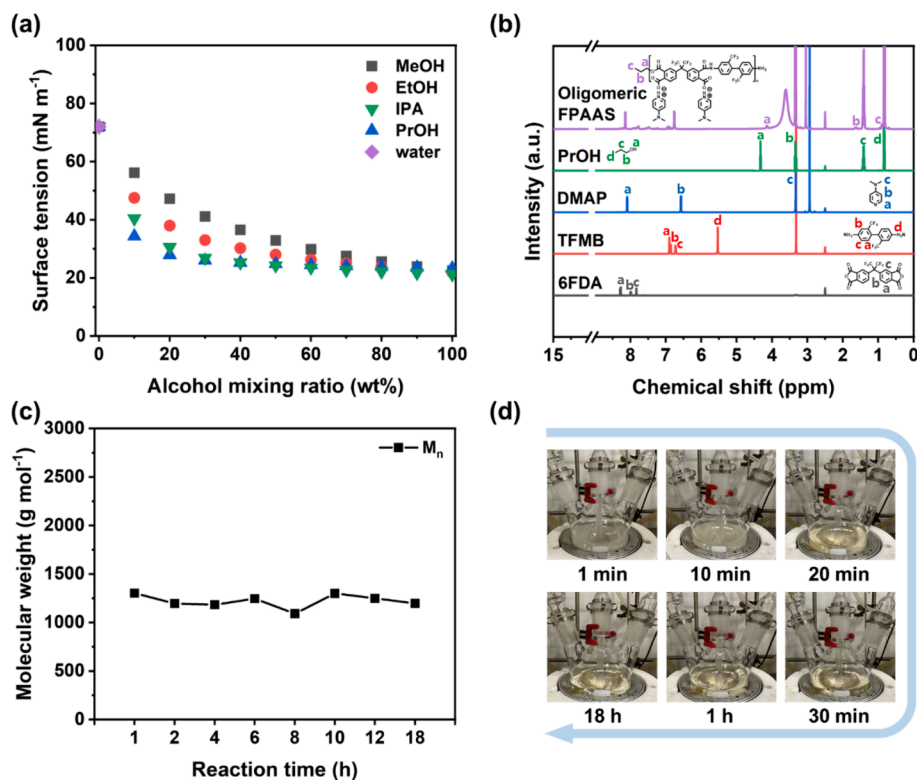


Fig. 2. Analysis of co-solvent systems optimization. (a) Surface tension variation with different alcohol mixing ratios in water. (b) ¹H NMR structural analysis of oligomeric FPAAS and reactants. (c) Molecular weight as a function of reaction time of oligomeric FPAAS. (d) Image of oligomeric FPAAS synthesis progress by reaction time.

Even with an extended reaction time of 18 h, there was minimal change in molecular weight, and a uniform and transparent solution was obtained (Fig. 2c,d). This signifies that the FPAAS reaction progresses rapidly and is successfully synthesized within one hour or less.

MALDI-TOF analysis was used in this study to measure the molecular weight precisely, which was initially estimated through GPC. The analysis revealed a precursor mixture with a molecular weight ranging from 850 to 2500 g mol⁻¹ (Fig. 3a). The results of the absolute molecular weight analysis, inferred from the ¹H NMR structural analysis highlighting the binding of 6FDA and PrOH to the terminal, provided insight into the molecular structure. Fig. 3b confirms the combination of 6FDA

and TFMB with PrOH attached to the end. This molecular structure and low molecular weight result from the combination of PrOH, acting as a solvent, with 6FDA. The ongoing reaction between the dianhydride and diamine produces a distinct structure. In contrast to the frequently produced high molecular weight PAAS precursors, PrOH binds to the end of the dianhydride, stopping the reaction and resulting in oligomeric FPAAS. All predicted structures for oligomeric FPAAS of various molecular weights are shown in Fig. S4.

The oligomeric FPAAS was prepared as described and then subjected to a thermal imidization process. Various analyses were performed to investigate the structural changes during this process, including ¹H

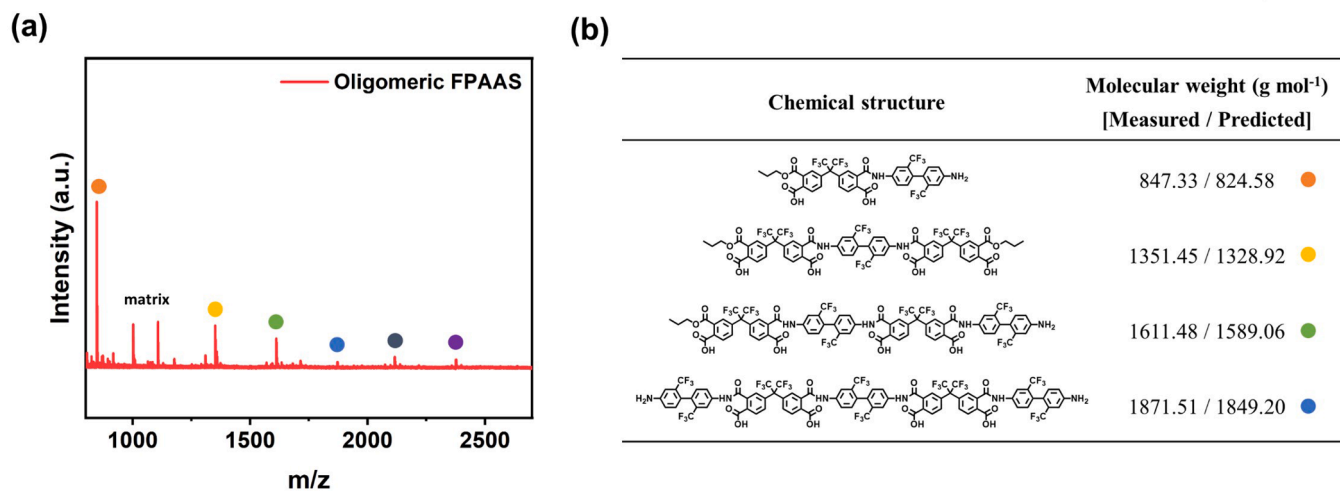


Fig. 3. Molecular weight analysis using 6FDA-TFMB@DMAP oligomeric FPAAS. (a) absolute molecular weight of oligomeric FPAAS using MALDI-TOF. (b) oligomeric FPAAS molecular structure predicted through absolute molecular weight.

NMR, degree of imidization, GPC, and GIWAXS. In contrast to general polyimides, which present analytical limitations due to their insoluble and infusible characteristics, the FPI prepared within this study is soluble due to its fluorine group, and thus was subjected to ^1H NMR and GPC analysis. The results are depicted in Fig. 4, and corresponding ^1H NMR and FT-IR spectra, along with GIWAXS profiles, for all analyzed segments are presented in Fig. S5. The ^1H NMR spectra indicate no structural changes up to 100 °C. The evaporation of solvent is indicated by a decrease in the PrOH signal at 0.9, 1.6, 3.3, and 4 ppm. The structural changes become evident upon reaching 150 °C, where the solvent has completely evaporated. The DMAP signals at 8.1, 6.7, and 3.0 ppm, which are stable up to 100 °C, display a slight shift upfield and a decrease in intensity. Simultaneously, a change in the peak shape of the benzene ring is observed. The imide peak becomes more prominent starting at 200 °C and reaches a complete imide structure at 300 °C, as depicted in Fig. 4a.

The results of the FT-IR analysis support those obtained from the NMR analysis, indicating a gradual decrease in the intensity of the PrOH hydroxyl peak at around $3,000\text{ cm}^{-1}$, which suggests solvent evaporation. Additionally, the imidization process that occurred between 150 °C

and 300 °C is confirmed by the increase in signals of C = O asymmetric stretching at 1784 cm^{-1} , C = O symmetric stretching at 1723 cm^{-1} , and imide C-N stretching at 1360 cm^{-1} , indicating the formation of an imide structure (Fig. 4b). The degree of imidization, which is calculated by measuring the change in the imide C-N bond at 1350 cm^{-1} , remains at zero up to 100 °C. It then increases rapidly at 150 °C and reaches complete imidization at 300 °C (Fig. 4c). Structural changes are also reflected in the molecular weight, as determined by GPC analysis (Fig. 4d). Up to 100 °C, there is no observable change in molecular weight, indicating the absence of structural changes. However, at 150 °C, a significant increase in molecular weight is observed reaching about $12,000\text{ g mol}^{-1}$. Subsequently, approximately $1,000\text{--}2,000\text{ g mol}^{-1}$ of the precursor oligomer converts to a polymer, and simultaneously, the imide ring forms. During this process, the molecular weight increases approximately 100-fold to about $90,000\text{ g mol}^{-1}$. The degree of polymerization can be quantified by measuring the change in molecular weight following the conversion of oligomeric FPAAS to FPI at elevated temperatures. Based on the GPC analysis of 6FDA-TFMB FPI, the molecular weight of the polymer chain is estimated to be approximately $90,000\text{ g mol}^{-1}$, while the molecular weight of the repeat unit is

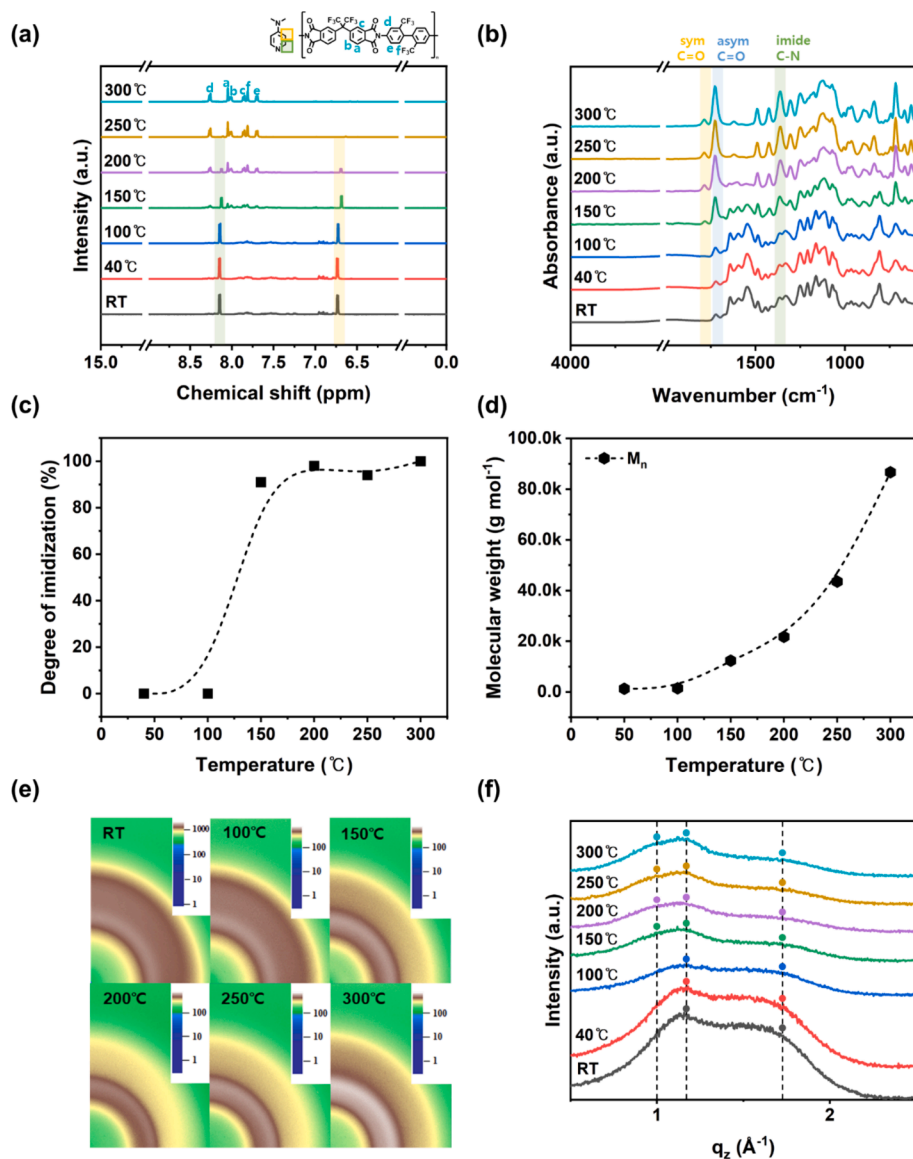


Fig. 4. Structural analysis of oligomeric FPAAS via thermal imidization step. (a) ^1H NMR. (b) FT-IR. (c) Degree of imidization. (d) GPC. (e) GIWAXS patterns of thin films prepared on silicon oxide substrates. (f) GIWAXS out-of-plane scattering profiles.

calculated to be $758.52 \text{ g mol}^{-1}$. Consequently, the degree of polymerization can be calculated to be approximately 118.

The trend is further confirmed by GIWAXS, where samples of oligomeric FPAAS were spin-coated on a silicon substrate at each step of thermal imidization. The GIWAXS results confirm that the in-plane and out-of-plane shapes are identical, as demonstrated by the complete semicircle shape (Fig. 4e). The out-of-plane GIWAXS scattering profiles are shown in Fig. 4f. Starting at 150°C , a scattering peak for a new structure is observed at $5.9\text{--}6.3 \text{ \AA}$, indicating that the short chain length oligomeric FPAAS is arranged more randomly than the long chain length FPI. The scattering peak at $5.9\text{--}6.3 \text{ \AA}$ corresponds to the peaks observed at 150°C , 200°C , 250°C , and 300°C above the dotted line at $q_z = 1$. This new packing mode suggests a higher molecular weight and slightly greater regularity than before, which supports the reasoning for solid-state polymerization mentioned previously. The analysis of the packing mode of the internal structure was performed with reference to the literature [42], and the d-spacing values for all peak positions in the graph are given in Table S2.

Based on the structural analyses conducted during thermal imidization, it is clear that the reactions in this study involve not only imidization but also novel polymerization within the thermal imidization process. As the solvent completely evaporates at lower temperatures during thermal imidization, the oligomeric FPAAS undergoes a new reaction as the temperature rises. This process follows a trajectory similar to conventional solid-state polymerization but diverges from existing polyimide solid-state polymerization methodologies.

Traditional polyimide production through solid-state polymerization involves forming powders, which requires high-temperature and high-pressure autoclaves for reacting monomer salts dispersed in water [43,44]. However, the new solid-state polymerization methods used in this study offer significant advantages. The production of oligomeric FPAAS can be achieved in less than an hour using this method, which is amenable to a solution approach with a uniform solution-type precursor, making processing straightforward. The use of water and alcohol as a co-solvent in the precursor synthesis aligns with an environmentally friendly approach. High molecular weight polyimides can be easily synthesized from precursors that do not require molecular weight control through solid-state polymerization during thermal imidization. This process was subjected to repeated testing, demonstrating excellent reproducibility (Table S3).

Furthermore, the salt-state precursors exhibit excellent storage stability. This was demonstrated through an analysis of the prepared FPI samples stored at room temperature and under frozen conditions for more than three weeks. The results confirmed that FPI manufactured from samples stored under both conditions for three weeks exhibited the same high molecular weight and well-formed structure (Fig. S6).

The physical properties of FPI films, prepared through solid-state polymerization, were comprehensively analyzed, as shown in Fig. 5. To evaluate the optical properties of the manufactured FPI, we compared the physical properties with experimental and literature values of a commercially available colorless polyimide film (L-3430 from Mitsubishi Gas Chemical) and 6FDA-TFMB-based FPI synthesized

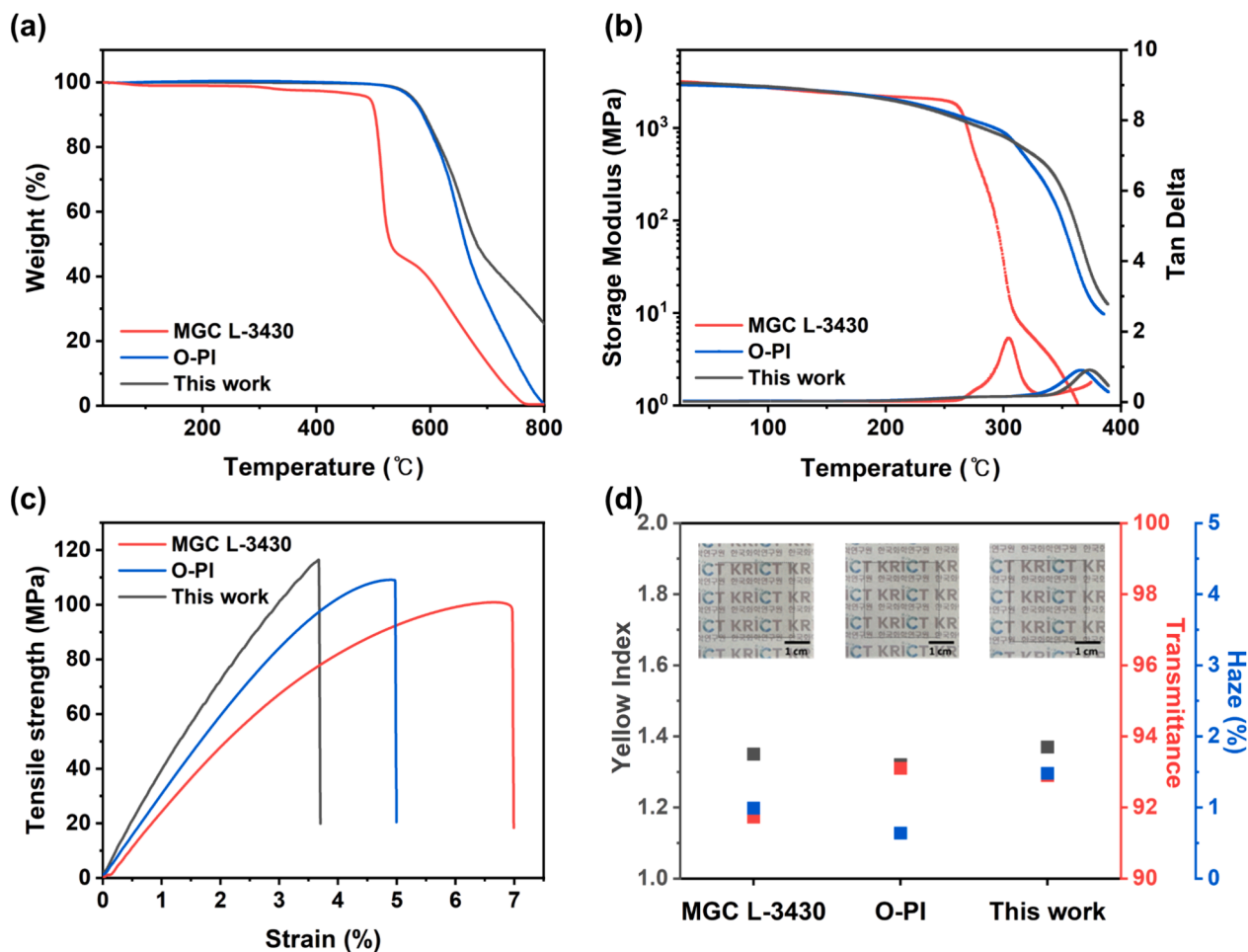


Fig. 5. Analysis of physical properties of fabricated polyimide films. (a) TGA thermogram. (b) Dynamic mechanical profile. (c) Stress-strain curve for mechanical property analysis. (d) Optical properties. The study compared various physical property analyses of the co-solvent based FPI fabricated in this study, the FPI fabricated with an organic solvent, and MGC's/L-3430 as comparison groups.

from an organic solvent of DMAc (O-FPI). Fig. S67 displays the analysis of O-FPI prepared using organic solvents. The ^1H NMR analysis confirmed the well-formed structures of the synthesized O-FPAA and O-FPI. Subsequently, GPC analysis confirmed the production of O-FPI equivalent to about $70,000 \text{ g mol}^{-1}$.

The thermal properties of FPI films were evaluated using TGA and DMA. The TGA analysis results in Fig. 5a show that the $T_{d,5\%}$ value is 570°C , indicating excellent stability even above 500°C . This indicates that the DMAP base, used to form the salt, was fully eliminated when compared to the oligomeric FPAAS curve in Fig. S8. Additionally, the DMA data in Fig. 5b confirms the excellent heat resistance of the fabricated FPI film, with a recorded T_g of 366.6°C . Compared to FPI films synthesized using organic solvents, the thermal properties were either equivalent or superior. The results of this study indicate that the thermal properties of the FPI film are superior to those of MGC's/L-3430 film. The mechanical properties of the FPI films were evaluated using UTM and the results are shown in the graph in Fig. 5c. The tensile strength was measured to be 116.5 MPa and the elongation at break was 3.7% . When compared to organic films of similar composition, it was confirmed to have almost equivalent values. However, the mechanical properties of general PI are somewhat superior to those of this material. This is because the charge transfer complex formed in FPI is suppressed compared to general PI, resulting in lower mechanical properties. These restrictions are due to the inherent mechanical limitations of the monomers used. To solve this problem, further improvements are needed, such as the preparation of composite PIs using monomers that can impart stiffness [45,46,47,48,49]. The optical properties of FPI films were evaluated using a spectrophotometer and a haze meter. The haze meter was used to measure the transmittance, which is the total transmittance over the wavelength range of 300 to 780 nm . According to the results shown in Fig. 5d, the yellow index of the $24 \mu\text{m}$ thick FPI film prepared in this study was determined to be 1.3 , with a transmittance of 92.9% and a haze value of 1.4% . These results indicate that the optical properties of the FPI films are comparable to those of Mitsubishi Gas Chemical's (MGC) L-3430 and FPI synthesized in organic solvents. The visual representations of the three films, namely MGC's/L-3430, FPI synthesized in organic solvents, and FPI synthesized in co-solvents, are shown next to the graph of the optical properties, excluding the literature values. The images clearly show that all three films were produced with transparent and uniform quality.

Table 1 presents a comprehensive comparison of the physical properties across four variants of fluorinated polyimides (FPIs). Utilizing a novel co-solvent system we developed, the oligomeric fluorinated poly(amic acid) salt (FPAAS) precursor was synthesized and subsequently processed into FPIs through solid-state polymerization and thermal imidization. The resulting FPIs exhibited physical properties that were

Table 1
Comparison of various 6FDA-TFMB based FPIs and physical properties.

		MGC ^a L-3430	O-PI ^b Ref ^c	O-PI	This work
Mechanical	Tensile strength (MPa)	100.9	99.4	109.1	116.5
	Elongation at break (%)	6.9	5.8	4.9	3.7
Thermal	$T_{d,5\%}$ ($^\circ\text{C}$)	493	541.8	567	570
	T_g ($^\circ\text{C}$)	306 (303)	351	365.9	366.6
Optical	Thickness (μm)	105	65.5	25	24
	Yellow index	1.35 (1.5)	1.3	1.32	1.37
	Transmittance (%)	91.7 (95.1)	89.7	93.1	92.9
	Haze (%)	0.9 (0.1)	1.7	0.64	1.4

(J): catalog value

^a MGC: Mitsubishi gas chemical Co. Ltd, Japan.

^b O-PI: polyimide synthesized from organic solvents of DMAc.

^c Ref. [50].

on par with those synthesized using conventional organic solvents, affirming the efficacy of our method in broadening the applicability of fluorine-based monomers in sustainable polymer synthesis.

To investigate the suitability of our method for various fluorine-based monomers, we introduced variations by keeping the dianhydride while expanding the diamine to include 2,2'-bis(trifluoromethyl) benzidine (TFMPDA) and 2-(trifluoromethyl)-1,4-phenylene diamine (6FpDA). The characterization of the FPI produced from the synthesized precursors and the thermal imidization process is described in detail in Fig. S9 and Fig. S10. The oligomeric FPAAS derived from 6FDA-TFMPDA@DMAP and 6FDA-6FpDA@DMAP exhibited a consistent low molecular weight of approximately 1200 g mol^{-1} , similar to the previous synthesis. Notably, ^1H NMR analysis confirmed the presence of PrOH signals attached to the end of 6FDA at 4.1 , 1.6 , and 0.9 ppm , affirming the molecular weight and structure achieved in the synthesis of oligomeric FPAAS. Furthermore, the molecular weight of the FPI produced through the thermal imidization process of FPAAS significantly increased compared to the previous case. This observation suggests that the same solid-state polymerization technique can be applied not only to FPI prepared with the earlier combination of 6FDA and TFMB but also to various monomers with fluorine-based substituents, such as TFMPDA and 6FpDA. The simplicity, convenience, and environmental friendliness of this solid-state polymerization method make it particularly noteworthy.

As the described FPIs provide remarkable optical transparency and thermal stability, a potential application includes transparent heaters for anti-fogging or anti-frosting devices. The application utilized polyimide made from commonly used fluorine-based monomers, 6FDA and TFMB. To demonstrate this point, AgNWs are coated on FPI substrates via a vacuum filtration transfer method, then, subsequently patterned via laser ablation [51,52] to fabricate FPI/AgNW heating devices. Briefly, AgNW inks with various concentrations can be vacuum-filtered, then can be physically transferred on top of a prepared FPI substrate. The resulting FPI/AgNW heaters provide optical transparency, as shown in Fig. 6a, based on a low-density percolation network with randomly oriented AgNWs (Fig. S11). As expected, a tradeoff relation is observed between optical transmittance (Fig. 6b) and electrical conductivity (Fig. 6c) by controlling AgNW density. For example, increasing AgNW density results in increasing conductivity with lower transmittance. For a quick note, FPI substrates maintain its original optical properties during the entire vacuum filtration transfer process including UV/ozone pretreatment for transfer AgNW electrodes (Fig. S12). Considering both optical transparency and electrical conductivity, a density of AgNW 120 mg m^{-2} was selected for transparent heating device applications.

The resulting FPI/AgNW heaters provide electrothermal heating (i. e., Joule heating) properties by applying electrical input voltage through AgNW-based percolation networks, as shown in Fig. 6d and Fig. S13. Based on the thermal stability of the FPI substrates, the heaters can be well-performed to increase the temperature up to 100°C under 9 V of electrical stimuli. To expand the utilization of the exceptional thermal properties of FPI substrates, the FPI/AgNW heaters can be further processed via selective laser ablation to pattern the AgNW electrodes. Using an IR pulse laser, the transferred AgNW networks can be selectively removed along the desired path without damaging the thermally stable FPI substrates, enabling spatially controlled patterning of the heaters, as shown in Fig. 6e and Fig. S14. The patterned heaters enable spatially controlled selective heating capabilities, thus, successful removal of fog at the desired wavy area can be achieved. As a brief summary, presented FPIs provide not only eco-friendly synthetic strategies but also versatile capabilities in many potential engineering applications.

4. Conclusion

In summary, we have developed an innovative, environmentally friendly synthesis method for fluorinated polyimides (FPIs) using a water-alcohol co-solvent approach. This method effectively addresses

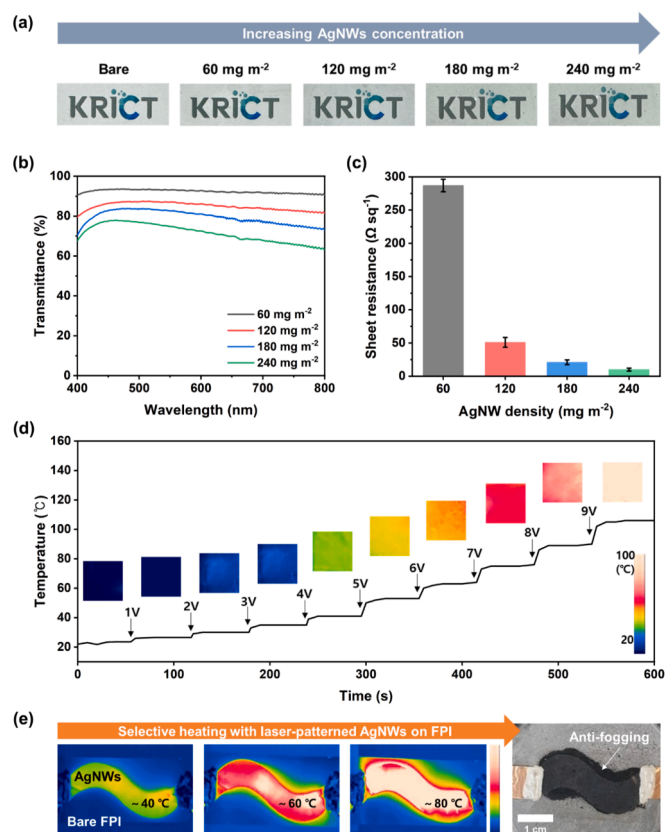


Fig. 6. Optical, electrical, and electrothermal heating properties of FPI/AgNW heaters. (a) A series of optical images showing optical transparency as a function of AgNW density. (b) Optical transmittance of FPI/AgNW heaters prepared by varying AgNW density. (c) Electrical sheet resistance of FPI/AgNW heaters prepared by varying AgNW density. (d) Electrothermal heating properties of FPI/AgNW heaters by increasing input voltage from 1 to 9 V. Insets show a series of IR images as a function of input voltage. (e) Spatially controlled selective heating of laser-patterned FPI/AgNW heaters and anti-fogging capability.

the environmental concerns associated with traditional organic solvents, presenting a sustainable alternative for FPI production. Our research successfully demonstrates the synthesis of oligomeric fluorinated poly(amic acid) salt (FPAAS) precursors, which exhibit robust hydrolytic stability and can be converted into high molecular weight FPI films through a novel solid-state polymerization and thermal imidization process. The FPI films obtained exhibit remarkable thermal stability, low yellow index, high transparency, and substantial tensile strength, which are comparable to those synthesized using conventional methods. Additionally, the use of FPI in the development of transparent heaters, with silver nanowire (AgNW) electrodes patterned via laser ablation, demonstrates the material's potential in creating anti-fogging or anti-frosting devices. These devices demonstrate exceptional electrothermal heating capabilities, reaching temperatures of up to 100 °C with a 9 V electrical stimulus, while maintaining both optical transparency and thermal stability. Additionally, our research expands the versatility of this synthesis approach to include monomers with various fluorine-based substituents, thereby broadening the scope of FPI applications. This approach offers the advantages of facile FPI synthesis without the need for meticulous molecular weight control, while adhering to environmentally friendly principles, which distinguishes it from traditional organic synthesis methods. In addition, the exceptional properties of the FPIs suggest a promising potential in many open opportunities in engineering applications.

Funding Sources

This study was supported by a KRICT Core Project (No. KS2421-20), the National Research Foundation of Korea (NRF-2021R1A2C2006771), and the Korea Evaluation Institute of Industrial Technology (KEIT) grant funded by the Ministry of Trade, Industry and Energy, Korea (KEIT-20024822).

6. Declaration of Generative AI and AI-assisted technologies in the writing process

During the preparation of this work the author(s) used DeepL in order to improve language. After using this tool/service, the author(s) reviewed and edited the content as needed and take(s) full responsibility for the content of the publication.

CRediT authorship contribution statement

Sarang Park: Writing – original draft, Methodology, Investigation, Formal analysis, Data curation. **Yujin So:** Methodology, Data curation, Conceptualization. **Ki Woong Kim:** Methodology, Investigation, Data curation. **Jongmin Park:** Writing – original draft, Methodology, Data curation. **Hyun Kim:** Writing – original draft, Supervision, Methodology, Data curation, Conceptualization. **Lee Kyung Kim:** Methodology, Investigation, Data curation. **Jinsoo Kim:** Validation, Data curation. **Hee-Tae Jung:** Supervision, Resources, Project administration. **Dae Woo Kim:** Validation, Supervision, Data curation. **Jong Chan Won:** Writing – original draft, Supervision, Resources, Conceptualization. **Yun Ho Kim:** Writing – review & editing, Writing – original draft, Supervision, Funding acquisition, Data curation, Conceptualization.

Declaration of competing interest

The authors declare that they have no known competing financial interests or personal relationships that could have appeared to influence the work reported in this paper.

Data availability

Data will be made available on request.

Appendix A. Supplementary data

Supplementary data to this article can be found online at <https://doi.org/10.1016/j.cej.2024.153288>.

References

- [1] D.J. Liaw, K.L. Wang, Y.C. Huang, K.R. Lee, J.Y. Lai, C.S. Ha, Advanced polyimide materials: Syntheses, physical properties and applications, *Prog. Polym. Sci.* 37 (2012) 907–974, <https://doi.org/10.1016/j.progpolymsci.2012.02.005>.
- [2] I. Gouzman, E. Grossman, R. Verker, N. Atar, A. Bolker, N. Eliaz, Advances in polyimide-based materials for space applications, *Adv. Mater.* 31 (2019) 1807738, <https://doi.org/10.1002/adma.201807738>.
- [3] Z. Xu, Z.L. Croft, D. Guo, K. Cao, G. Liu, Recent development of polyimides: Synthesis, processing, and application in gas separation, *J. Polym. Sci.* 59 (2021) 943–962, <https://doi.org/10.1002/pol.20210001>.
- [4] Z. Wu, J. He, H. Yang, S. Yang, Progress in aromatic polyimide films for electronic applications: Preparation, structure and properties, *Polym.* 14 (2022) 1269, <https://doi.org/10.3390/polym14061269>.
- [5] Y. Li, G. Sun, Y. Zhou, G. Liu, J. Wang, S. Han, Progress in low dielectric polyimide film—A review, *Prog. Org. Coat.* 172 (2022) 107103, <https://doi.org/10.1016/j.porgcoat.2022.107103>.
- [6] W. Zheng, T. Yang, L. Qu, X. Liang, C. Liu, C. Qian, T. Zhu, Z. Zhou, C. Liu, S. Liu, Z. Chi, J. Xu, Y. Zhang, Temperature resistant amorphous polyimides with high intrinsic permittivity for electronic applications, *Chem. Eng. J.* 436 (2022) 135060, <https://doi.org/10.1016/j.cej.2022.135060>.
- [7] S. Huang, X. Lv, X. Lai, J. Li, Y. Zhang, S. Qiu, G. Zhang, R. Sun, A strategy to prepare low-temperature curable photosensitive polyimide with good comprehensive performance, *Chem. Eng. J.* 477 (2023) 146858, <https://doi.org/10.1016/j.cej.2023.146858>.

- [8] G. Hougham, G. Tesoro, J. Shaw, Synthesis and properties of highly fluorinated polyimides, *Macromol.* 27 (1994) 3642–3649, <https://doi.org/10.1021/ma00091a028>.
- [9] S.-J. Park, K.S. Cho, S.H. Kim, A study on dielectric characteristics of fluorinated polyimide thin film, *J. Colloid. Interface. Sci.* 272 (2004) 384–390, <https://doi.org/10.1016/j.jcis.2003.12.027>.
- [10] C. Wang, S. Cao, W. Chen, C. Xu, X. Zhao, J. Li, Q. Ren, Synthesis and properties of fluorinated polyimides with multi-bulky pendant groups, *RSC Adv.* 7 (2017) 26420–26427, <https://doi.org/10.1039/C7RA01568B>.
- [11] T. Xiao, X. Fan, D. Fan, Q. Li, High thermal conductivity and low absorptivity/emissivity properties of transparent fluorinated polyimide films, *Polym. Bull.* 74 (2017) 4561–4575, <https://doi.org/10.1007/s00289-017-1974-6>.
- [12] A.X. Wu, J.A. Drayton, K.M. Rodriguez, Q. Qian, S. Lin, Z.P. Smith, Influence of aliphatic and aromatic fluorine groups on gas permeability and morphology of fluorinated polyimide films, *Macromol.* 53 (2020) 5085–5095, <https://doi.org/10.1021/acs.macromol.0c01024>.
- [13] H. Li, J. Liu, K. Wang, L. Fan, S. Yang, Synthesis and characterization of novel fluorinated polyimides derived from 4, 4'-[2, 2, 2-trifluoro-1-(3, 5-difluoromethylphenyl) ethylenediphenyl] anhydride and aromatic diamines, *Polym.* 47 (2006) 1443–1450, <https://doi.org/10.1016/j.polymer.2005.12.074>.
- [14] Z. Mi, Z. Liu, J. Yao, C. Wang, C. Zhou, D. Wang, X. Zhao, H. Zhou, Y. Zhang, C. Chen, Transparent and soluble polyimide films from 1, 4: 3, 6-dianhydro-D-mannitol based dianhydride and diamines containing aromatic and semiaromatic units: Preparation, characterization, thermal and mechanical properties, *Polym. Degrad. Stab.* 151 (2018) 80–89, <https://doi.org/10.1016/j.polymerdegradstab.2018.01.006>.
- [15] W. Xu, Y. Su, M. Shang, X. Lu, Q. Lu, Rapid synthesis of polyimide precursors by solution polymerization using Continuous-flow microreactors, *Chem. Eng. J.* 397 (2020) 125361, <https://doi.org/10.1016/j.cej.2020.125361>.
- [16] S. Chu, Y. Wang, Y. Guo, P. Zhou, H. Yu, L. Luo, F. Kong, Z. Zou, Facile green synthesis of crystalline polyimide photocatalyst for hydrogen generation from water, *J. Mater. Chem.* 22 (2012) 15519–15521, <https://doi.org/10.1039/C2JM32595K>.
- [17] Y. Alqaheem, A. Alomair, A. Alhendi, S. Alkandari, N. Tanoli, N. Alnajdi, A. Quesada-Peréz, Preparation of polyetherimide membrane from non-toxic solvents for the separation of hydrogen from methane, *Chem. Cent. J.* 12 (2018) 1–8, <https://doi.org/10.1186/s13065-018-0449-7>.
- [18] S. Ghaffari-Mosanezhadeh, O.A. Tafreshi, S. Karamikamkar, Z. Saadatnia, E. Rad, M. Meysami, H.E. Naguib, Recent advances in tailoring and improving the properties of polyimide aerogels and their application, *Adv. Colloid. Interface. Sci.* 304 (2022) 102646, <https://doi.org/10.1016/j.cis.2022.102646>.
- [19] L.S. Soh, S.U. Hong, C.Z. Liang, W.F. Yong, Green solvent-synthesized polyimide membranes for gas separation: Coupling Hansen solubility parameters and synthesis optimization, *Chem. Eng. J.* 478 (2023) 147451, <https://doi.org/10.1016/j.cej.2023.147451>.
- [20] D. Cai, J. Su, M. Huang, Y. Liu, J. Wang, L. Dai, Synthesis, characterization and hydrolytic stability of poly (amic acid) ammonium salt, *Polym. Degrad. Stab.* 96 (2011) 2174–2180, <https://doi.org/10.1016/j.polymerdegradstab.2011.09.008>.
- [21] L. Weng, H.X. Li, X.P. Yang, L.Z. Liu, Preparation and characterization of silica/polyimide nanocomposite films based on water-soluble poly (amic acid) ammonium salt, *Polym. Compos.* 38 (2017) 774–781, <https://doi.org/10.1002/pc.23637>.
- [22] T. Kim, B. Park, K.M. Lee, S.H. Joo, M.S. Kang, W.C. Yoo, S.K. Kwak, B.S. Kim, Hydrothermal synthesis of composition- and morphology-tunable polyimide-based microparticles, *ACS Macro Lett.* 7 (2018) 1480–1485, <https://doi.org/10.1021/acsmacrolett.8b00680>.
- [23] S.W. Jin, Y.J. Choi, H.C. Yu, S.H. Lee, Y.J. Jin, I.S. Lee, H.S. Lee, C.M. Chung, Preparation of polyimide powders via hydrothermal polymerization and post-heat treatment for application to compression-molding materials, *ACS Sustain. Chem. Eng.* 10 (2022) 1910–1919, <https://doi.org/10.1021/acssuschemeng.1c07621>.
- [24] T. Kim, S.H. Joo, J. Gong, S. Choi, J.H. Min, Y. Kim, G. Lee, E. Lee, S. Park, S. K. Kwak, H.S. Lee, B.S. Kim, Geomimetic Hydrothermal Synthesis of Polyimide-Based Covalent Organic Frameworks, *Angew. Chem. Int. Ed.* 61 (2022) e202113780.
- [25] J. Chiefari, B. Dao, A.M. Groth, J.H. Hodgkin, Water as solvent in polyimide synthesis: Thermoset and thermoplastic examples, *High Perform. Polym.* 15 (2003) 269–279, <https://doi.org/10.1177/0954008303015003004>.
- [26] J. Yang, M.H. Lee, A water-soluble polyimide precursor: Synthesis and characterization of poly (amic acid) salt, *Macromol. Res.* 12 (2004) 263–268, <https://doi.org/10.1007/BF03218398>.
- [27] J. Chiefari, B. Dao, A.M. Groth, J.H. Hodgkin, Water as solvent in polyimide synthesis II: Processable aromatic polyimides, *High Perform. Polym.* 18 (2006) 31–44, <https://doi.org/10.1177/0954008306055181>.
- [28] J. Chiefari, B. Dao, A.M. Groth, J.H. Hodgkin, Water as solvent in polyimide synthesis III: Towards the synthesis of polyamideimides, *High Perform. Polym.* 18 (2006) 437–451, <https://doi.org/10.1177/0954008306064906>.
- [29] Z. Cao, X. Zhao, D. Wang, C. Chen, C. Qu, C. Liu, X. Hou, L. Li, G. Zhu, Polymerization of poly-(amic acid) ammonium salt in aqueous solution and its use in flexible printed circuit boards, *Eur. Polym. J.* 96 (2017) 393–402, <https://doi.org/10.1016/j.eurpolymj.2017.09.023>.
- [30] H. Zhou, S. Zheng, C. Liu, C. Qu, Y. Wang, W. Xiao, H. Li, D. Zhao, J. Chang, Preparation and characterization of high-performance polyamic acid salt hydrogel in aqueous solution, *High Perform. Polym.* 31 (2019) 497–502, <https://doi.org/10.1177/0954008318818885>.
- [31] Y. Jeong, H. Park, Y. So, H.J. Mun, T.J. Shin, N.K. Park, J. Kim, S. Yoo, J.C. Won, Y. H. Kim, Enhanced hydrolytic and electrical stability of eco-friendly processed polyimide gate dielectrics for organic transistors, *J. Mater. Chem. C* 8 (2020) 14370–14377, <https://doi.org/10.1039/D0TC03341C>.
- [32] C. Wang, S. Ma, D. Li, J. Zhao, H. Zhou, D. Wang, D. Zhou, T. Gan, D. Wang, C. Liu, C. Qu, C. Chen, 3D printing of lightweight polyimide honeycombs with the high specific strength and temperature resistance, *ACS Appl. Mater. Interfaces* 13 (2021) 15690–15700, <https://doi.org/10.1021/acsami.1c01992>.
- [33] S. Zheng, L. Jiang, C. Zhang, N. Ma, X. Liu, Facile and environment-friendly preparation of high-performance polyimide aerogels using water as the only solvent, *Polym. Chem.* 13 (2022) 2375–2382, <https://doi.org/10.1039/D1PY01573G>.
- [34] S. Kim, Y. Lee, J. Park, Y. So, H.T. Jung, M.J. Ko, J.C. Won, S. Jeong, Y.H. Kim, Green and facile synthesis of hybrid composites with ultralow dielectric properties from water-soluble polyimide and dual-porous silica nanoparticles, *ACS Appl. Mater. Interfaces* 15 (2022) 4408–4418, <https://doi.org/10.1021/acsami.2c16197>.
- [35] J.C. Biffinger, H.W. Kim, S.G. DiMaggio, The polar hydrophobicity of fluorinated compounds, *ChemBioChem* 5 (2004) 622–627, <https://doi.org/10.1002/cbic.200300910>.
- [36] P. Lee, J. Lee, H. Lee, J. Yeo, S. Hong, K.H. Nam, D. Lee, S.S. Lee, S.H. Ko, Highly stretchable and highly conductive metal electrode by very long metal nanowire percolation network, *Adv. Mater.* 24 (2012) 3326–3332, <https://doi.org/10.1002/adma.201200359>.
- [37] J.V. Facinelli, S.L. Gardner, L. Dong, C.L. Sensenig, R.M. Davis, J.S. Riffle, Controlled molecular weight polyimides from poly (amic acid) salt precursors, *Macromol.* 29 (1996) 7342–7350, <https://doi.org/10.1021/ma960885s>.
- [38] J.C. Johnston, M.A.B. Meador, W.B. Alston, A mechanistic study of polyimide formation from diester-diacids, *J. Polym. Sci. Part A: Polym. Chem.* 25 (1987) 2175–2183, <https://doi.org/10.1002/pola.1987.080250814>.
- [39] Korea Research Institute of Chemical Technology, Aqueous polyamic acid composition, KR Patent 10-2644737-0000, Korean Intellectual Property Office, Daejeon, 2024.
- [40] Y. Miyako, N. Khalef, K. Matsuzaki, R. Pinal, Solubility enhancement of hydrophobic compounds by cosolvents: role of solute hydrophobicity on the solubilization effect, *Int. J. Pharm.* 393 (2010) 48–54, <https://doi.org/10.1016/j.ijpharm.2010.03.059>.
- [41] G. Vazquez, E. Alvarez, J.M. Navaza, Surface tension of alcohol water+ water from 20 to 50. degree. C, *J. Chem. Eng. Data* 40 (1995) 611–614, <https://doi.org/10.1021/je00019a016>.
- [42] J. Wakita, S. Jin, T.J. Shin, M. Ree, S. Ando, Analysis of molecular aggregation structures of fully aromatic and semialiphatic polyimide films with synchrotron grazing incidence wide-angle X-ray scattering, *Macromol.* 43 (2010) 1930–1941, <https://doi.org/10.1021/ma902252y>.
- [43] M.M. Unterlass, F. Emmerling, M. Antonietti, J. Weber, From dense monomer salt crystals to CO 2 selective microporous polyimides via solid-state polymerization, *Chem. Commun.* 50 (2014) 430–432, <https://doi.org/10.1039/C3CC47674J>.
- [44] B. Baumgartner, M. Puchberger, M.M. Unterlass, Towards a general understanding of hydrothermal polymerization of polyimides, *Polym. Chem.* 6 (2015) 5773–5781, <https://doi.org/10.1039/C5PY00231A>.
- [45] C.P. Yang, Y.Y. Su, Y.C. Chen, Light-colored fluorinated polyimides based on 2, 5-bis (4-amino-2-trifluoromethylphenoxy) biphenyl and various aromatic dianhydrides, *J. Appl. Polym. Sci.* 102 (2006) 4101–4110, <https://doi.org/10.1002/app.24118>.
- [46] C.H. Choi, B.H. Sohn, J.H. Chang, Colorless and transparent polyimide nanocomposites: Comparison of the properties of homo- and co-polymers, *J. Ind. Eng. Chem.* 19 (2013) 1593–1599, <https://doi.org/10.1016/j.jiec.2013.01.028>.
- [47] X. Ye, P. Gong, J. Wang, H. Wang, S. Ren, S. Yang, Fluorinated graphene reinforced polyimide films with the improved thermal and mechanical properties, *Compos. Part A: Appl. Sci. Manuf.* 75 (2015) 96–103, <https://doi.org/10.1016/j.compositesa.2015.04.005>.
- [48] P. Zhang, J. Zhao, K. Zhang, R. Bai, Y. Wang, C. Hua, Y. Wu, X. Liu, H. Xu, Y. Li, Fluorographene/polyimide composite films: mechanical, electrical, hydrophobic, thermal and low dielectric properties, *Compos. Part A: Appl. Sci. Manuf.* 84 (2016) 428–434, <https://doi.org/10.1016/j.compositesa.2016.02.019>.
- [49] Y. Xu, M. Zhang, Y. Pang, T. Zheng, C. Tian, Z. Wang, J. Yan, Colorless polyimide copolymers derived from isomeric biphenyltetracarboxylic dianhydrides and 2, 2'-bis (trifluoromethyl) benzidine, *Eur. Polym. J.* 193 (2023) 112099, <https://doi.org/10.1016/j.eurpolymj.2023.112099>.
- [50] J.J. He, H.X. Yang, F. Zheng, S.Y. Yang, Dielectric properties of fluorinated aromatic polyimide films with rigid polymer backbones, *Polym.* 14 (2022) 649, <https://doi.org/10.3390/polym14030649>.
- [51] S. Hong, J. Yeo, J. Lee, H. Lee, P. Lee, S.S. Lee, S.H. Ko, Selective laser direct patterning of silver nanowire percolation network transparent conductor for capacitive touch panel, *J. Nanosci. Nanotechnol.* 15 (2015) 2317–2323, <https://doi.org/10.1166/jnn.2015.9493>.
- [52] S. Hong, H. Lee, J. Lee, J. Kwon, S. Han, Y.D. Suh, H. Cho, J. Shin, J. Yeo, S.H. Ko, Highly stretchable and transparent metal nanowire heater for wearable electronics applications, *Adv. Mater.* 27 (2015) 4744–4751, <https://doi.org/10.1002/adma.201500917>.